



OXFORD CENTRE FOR COLLABORATIVE APPLIED MATHEMATICS

Report Number 09/21

**A finite difference method for free boundary
problems**

by

Bengt Fornberg



Oxford Centre for Collaborative Applied Mathematics
Mathematical Institute
24 - 29 St Giles'
Oxford
OX1 3LB
England

A FINITE DIFFERENCE METHOD FOR FREE BOUNDARY PROBLEMS

BENGT FORNBERG*

Abstract. Fornberg and Meyer-Spasche proposed some time ago a simple strategy to correct finite difference schemes in the presence of a free boundary that cuts across a Cartesian grid. We show here how this procedure can be combined with a minimax-based optimization procedure to rapidly solve a wide range of elliptic-type free boundary value problems.

Key words. Finite differences, free boundary, minimax optimization.

1. Introduction. Both free and moving boundary problems arise in a vast number of physical settings, as surveyed for example in [3] and [10]. We focus in this study on free boundary (FB) problems of the type

$$Lu + f^+(u) = 0 \tag{1.1}$$

where L is a linear (or locally linearizable) second order elliptic differential operator, and

$$f^+(u) = \begin{cases} \lambda u + O(u^2) \text{ or } \mu + O(u) & \text{if } u > 0 \\ 0 & \text{if } u \leq 0 \end{cases} . \tag{1.2}$$

Here u is a function of any number of space variables, and λ and μ are either constants or smooth functions of the space variables. The many important FB problems that can be cast in these forms include the Euler equations for steady flows [4] and the Grad-Shafranov equation describing magnetohydrodynamic (MHD) equilibria in plasma physics [1], [7].

The simplest possible numerical approach for the present class of problems would be to discretize L with standard second order finite difference (FD2) approximations (a 5-point stencil in 2-D if L contains no mixed derivatives), and use for $f^+(u)$ its value at the FD2-stencil's center point. The two main problems with this approach are how to:

- Avoid the loss of accuracy that will arise because of inaccurate treatment of the interface on the fixed grid. Movements of the FB with less than the grid spacing may not be 'felt' at all by this numerical scheme.

An extremely simple correction scheme (involving no u -values beyond those that are already part of the basic FD2 stencil) was initially proposed in [9], and then discussed further in [8]. Like for the immersed interface method [6], second order accurate results are obtained starting with standard FD2 approximations of L . We will find here that the FB influence in some cases will be sufficiently reduced that Richardson extrapolation can be used to improve the accuracy still further.

- Achieve a high and reliable rate of convergence in the numerical iterations.

Since FB problems are nonlinear, some type of iterative scheme will be needed for their solution. Successful options include a regula falsi approach [5],

*University of Colorado, Department of Applied Mathematics, 526 UCB, Boulder, CO 80309, USA (fornberg@colorado.edu).

Newton-type iterations [2], and fixed-area (or fixed-circulation) functional iterations [4]. We propose here the use of a numerical ‘minimax’ approach, implemented for example with the *fminimax* function in Matlab’s optimization toolbox.

We introduce in Section 2 two test problems that were earlier considered in [8], and then proceed by

- Describing the FB correction procedure,
- Showing how this procedure reduces the numerical residual in case both the FB and the analytic solution u is known,
- Showing how we can obtain an accurate solution to u in case only the free boundary is given, and how this provides an easy-to-measure residual if the given boundary approximation is inaccurate,
- Showing how the FB approximation can be adjusted in order to minimize this residual.

The last of these steps amounts to a very short and easy-to-implement Cartesian grid-based FD2 algorithm in which the presence of a FB only leads to a very small degradation of accuracy.

2. Two primary test problems. After having arrived at the numerical procedure in Section 6, we will use Problems 1 and 2 described below for the numerical tests given in Section 7. Euler flows give rise to FB equations of a similar type as Problem 1 while both types frequently arise in MHD contexts (tokamaks, solar physics, etc.). The task will be to numerically determine both the PDE solution $u(x, y)$ and the FB. The solution $u(x, t)$ to Problem 1 will feature a discontinuous second derivative at the FB. The solution to Problem 2 is one order smoother - irregular first in its third derivative. Although this is not a limitation of the numerical approach, we restrict for simplicity our attention to problems in which the FB does not intersect any fixed boundary or any edge of the computational domain.

2.1. Problem 1. Consider the PDE

$$\frac{\partial^2 u}{\partial x^2} + \frac{\partial^2 u}{\partial y^2} + H(u) = 0 \quad (2.1)$$

where

$$H(u) = \begin{cases} 1 & \text{if } u > 0 \\ 0 & \text{if } u \leq 0 \end{cases}.$$

We will solve this elliptic FB problem over $-4 \leq x \leq 4$, $-4 \leq y \leq 4$ with boundary conditions (BC) along the four sides that match the analytic solution

$$u(x, y) = \begin{cases} 1 - r^2/4 & \text{if } r < 2 \\ 2 \ln(2/r) & \text{if } r \geq 2 \end{cases}, \quad (2.2)$$

where $r = \sqrt{x^2 + y^2}$.

2.2. Problem 2. Consider the PDE

$$\frac{\partial^2 u}{\partial x^2} + \frac{\partial^2 u}{\partial y^2} + u^+ = 0 \quad (2.3)$$

with

$$u^+ = \begin{cases} u & \text{if } u > 0 \\ 0 & \text{if } u \leq 0 \end{cases}.$$

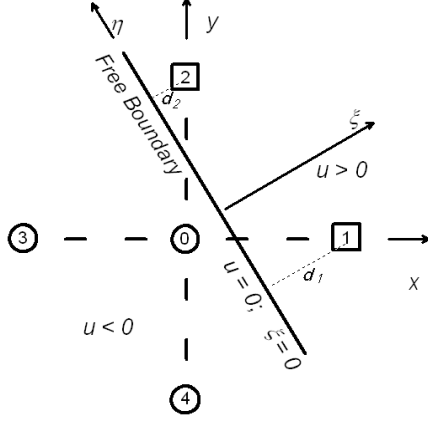


FIG. 3.1. Schematic illustration of a FB cutting across two legs of a 2-D 5-point stencil. The nodes marked 1 and 2 fall here on the opposite side of the FB than the stencil center point (node 0).

In this case, the analytical solution is

$$u(x, y) = \begin{cases} J_0(r) & \text{if } r < r_c \\ A \ln(r_c/r) & \text{if } r \geq r_c \end{cases} . \quad (2.4)$$

The radius r is defined as before, $r_c \approx 2.404826$ is the first zero of $J_0(r)$, and $A = r_c J_1(r_c) \approx 1.248459$.

3. Concept behind the FB correction procedure. We start by considering Problem 1, and assume at first that we know both $u(x, y)$ and the location of the FB (along which $u = 0$). Standard FD2 approximations will be locally second order accurate (in the grid spacing h) whenever the FB does not cut across any of the four legs of the 5-point FD2 stencil. Consider next the situation in Figure 3.1 and let u_k denote the u -value at node k , $k = 0, 1, \dots, 4$. We have in this case $u_0 < 0$, and the standard FD approximation becomes

$$(u_1 + u_2 + u_3 + u_4 - 4u_0) \frac{1}{h^2} = 0. \quad (3.1)$$

Locally approximating the FB by a straight line, we can introduce the (ξ, η) -system that is also shown in the figure. In this system, the PDE simplifies to

$$u_{\xi\xi} = \begin{cases} 0 & \text{where } \xi < 0 \\ -1 & \text{where } \xi > 0 \end{cases} . \quad (3.2)$$

The values of u at the nodes 1 and 2 are therefore smaller than what they otherwise would have been by the amounts $\frac{1}{2}d_1^2$ and $\frac{1}{2}d_2^2$, respectively, where d_1 and d_2 are the distances by which these nodes fall outside the FB. If we subtract $\frac{1}{2h^2}d_1^2 + \frac{1}{2h^2}d_2^2$ from the right hand side (RHS) of (3.1), local second order accuracy becomes restored. If only one leg of a stencil extends across the FB, we similarly need only one correction term of this kind. If the stencil center falls in the region where $u > 0$, any stencil leg that extends across the FB can likewise be corrected by just reversing the sign of the correction term. All that needs to be kept track of is therefore the distances between the FB and any nodes that fall on the other side of it relative to the stencil's center point (or some approximations for these distances).

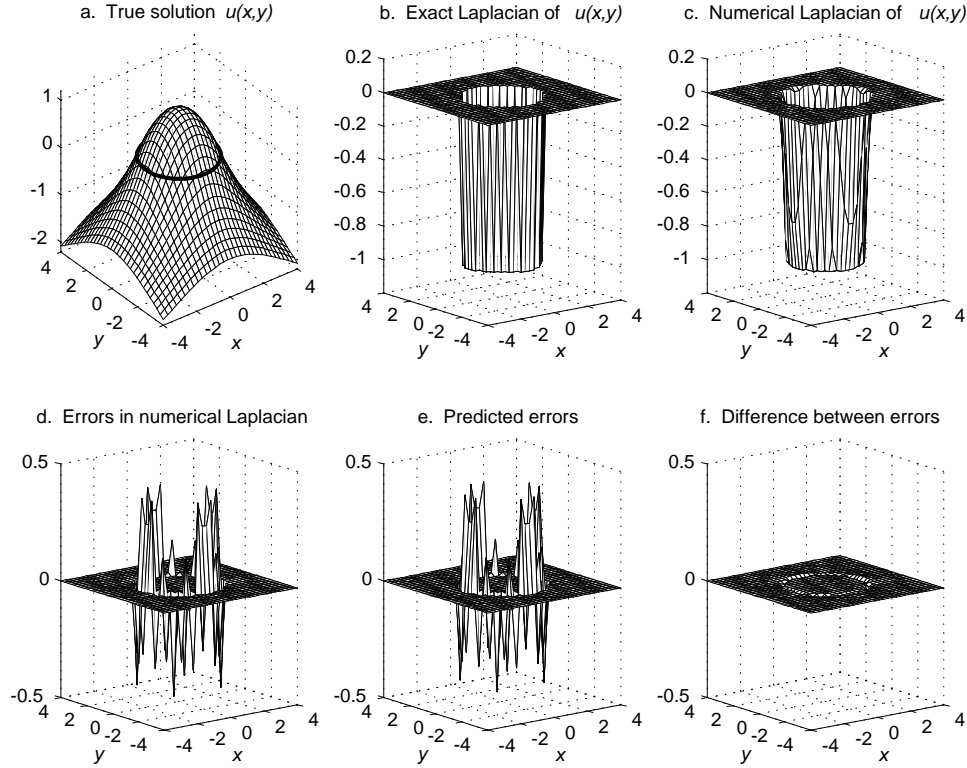


FIG. 4.1. The true solution to Problem 1 on a 32×32 grid; Laplacians and residuals without and with the correction procedure.

4. Calculation of the finite difference (FD) residual if the correct PDE solution and the FB are given. The top row of subplots in Figure 4.1 displays, from left to right, (a) the analytic solution (2.2) (with the FB marked), (b) the analytic Laplacian at all node points (taking the value -1 when $r < 2$, zero otherwise), and (c) the numerical Laplacian, as obtained by applying the 5-point stencil to the analytic solution at all node points. Superficially, the two last plots look quite similar, but the first subplot in the bottom row (d) reveals that they in fact differ quite dramatically and in a highly irregular manner along the FB. Subplot (e) displays what the correction procedure above tells that the RHS ought to have been adjusted with in order to account for the FB. The excellent agreement between the latter two results is confirmed in subplot (f), which shows their difference. The correction procedure has indeed predicted very accurately the error introduced by the FB

5. Calculation of the PDE solution if the FB is given. We next assume that only the FB is given, but not the solution $u(x,t)$. Based on knowing the FB, we can trivially detect when one or two legs of a stencil extends across it and adjust the PDE's RHS accordingly. Figure 5.1 shows in subplot (a) the FD2 solution to the PDE if the corrections are not made, and in subplot (b) its difference to the analytical solution (2.2). With the correction included, subplot (c) shows that the errors due to the FB have been virtually eliminated. The discrepancies that remain come from standard second order truncation errors in the smooth regions. In Figure 5.2, we

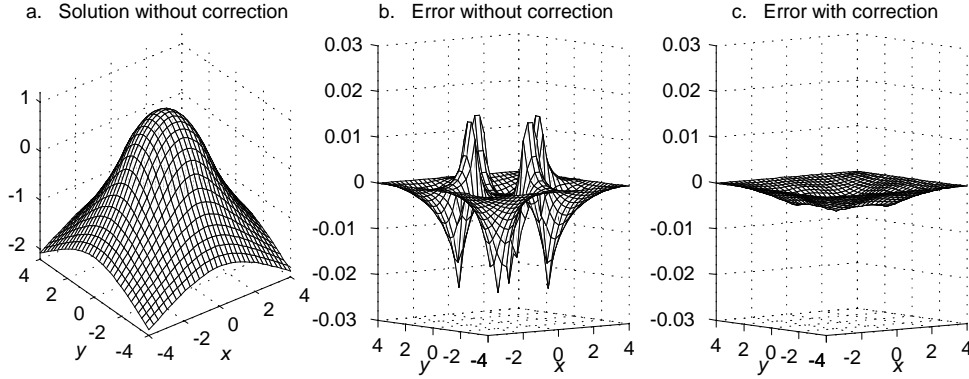


FIG. 5.1. Numerical solution to Problem 1 when the FB is given; errors without and with the correction procedure.

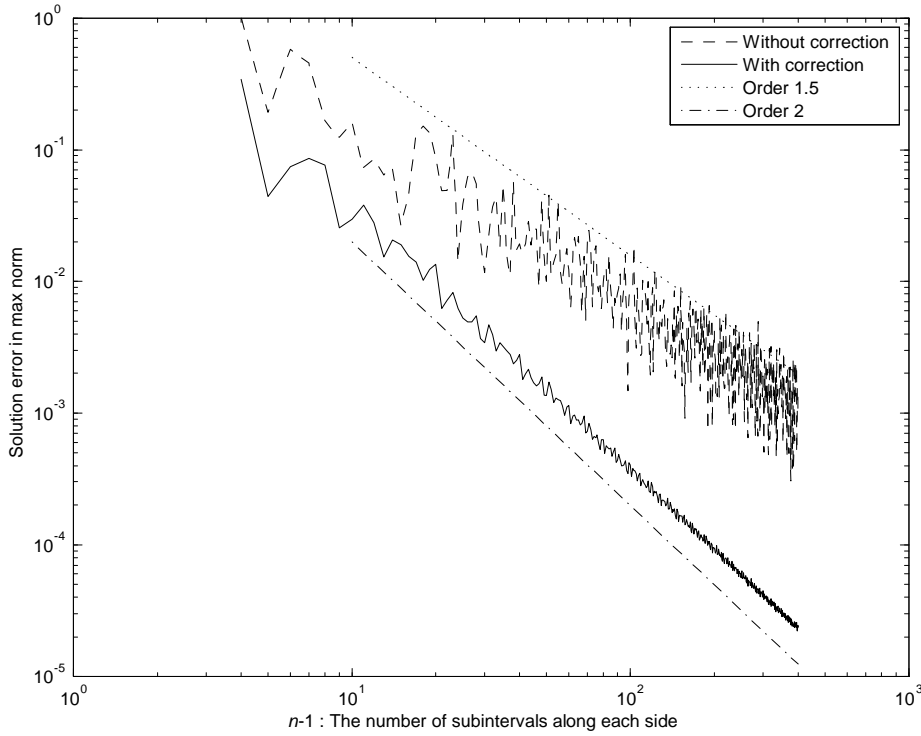


FIG. 5.2. Max norm errors when solving Problem 1 with the FB location given. The step size h satisfies $h = 8/(n - 1)$.

display the solution errors, in max norm over all the node points when we, instead of a 32×32 grid, use $n \times n$ grids, where n ranges from 5 to 401. Without correction, the error is seen to be highly erratic, roughly following an $O(h^{1.5})$ trend. It would have been $O(h^1)$ had it not been for the cancellations due to the randomly varying signs of the errors, as seen in Figure 4.1 (d). With the correction approach in place, the solid curve in Figure 5.2 very clearly shows the error trend to instead be $O(h^2)$,

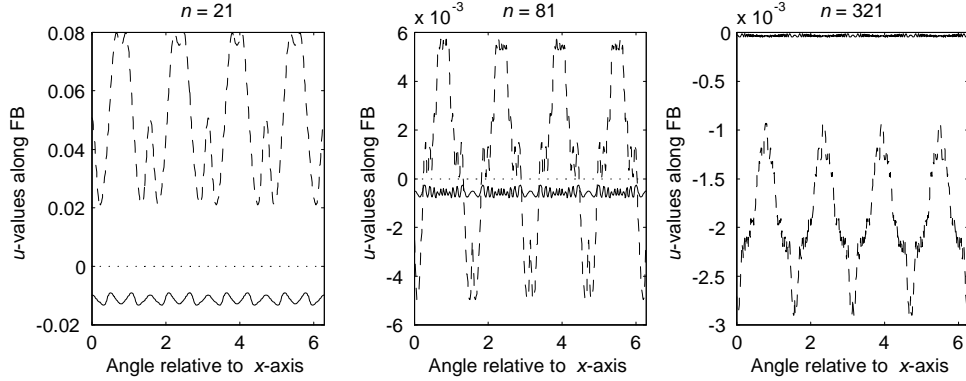


FIG. 6.1. Values of $u(x,y)$ along the FB (given - here parametrized by the angle in polar coordinates). Dashed line: without the correction, solid line: with correction. The ideal curves should be identically zero - marked by a dotted line. As before, n denotes the number of nodes along each side.

just as would have been the case if no FB had been present. To reach an error level of 10^{-3} , $n \approx 100$ suffices when the correction method is used vs. $n \approx 1000$ otherwise - a saving with a factor of 100 in total number of nodes.

6. Adjusting the FB to minimize the residual. Numerical algorithm.

When the FB is given, we saw in the last section how we then readily can calculate the full solution $u(x,y)$. In particular, it is then easy (for example with Matlab's *interp2* routine) to inspect u along the FB. Ideally, in the absence of errors in both the FB location and in the numerical FD2 approximation, this ought to produce a perfectly zero result. When using the analytically correct FB, the subplots of Figure 6.1 show the numerically obtained values along it (displayed at equispaced angles, as seen from the origin) when $n = 21, 81, 321$. In each case, the solid curve shows the result with the FB correction in use, and the dashed curve without it. A thin dotted line marks the desired zero error level (overlapping with the top of the display frame in the last case). The errors without the correction procedure are far greater than with it.

We are now ready to describe our proposed strategy for when neither the solution $u(x,y)$, nor the FB are provided. The only two components that are needed are:

- A routine which, given a FB, returns the residual (accurate computed values of $u(x,y)$) along it.
- An optimization routine, such as Matlab's *fminimax*, to vary the parameters describing the FB in such a way that this residual gets minimized.

Since a FBs tend to be very smooth in the present problem class, some 6-10 free parameters usually suffices to describe them well (e.g. Fourier coefficients if the FB is represented in polar form, or sample points along the FB in case we use periodic splines). We smooth out the high frequency noise in the residuals and then sample the smoothed residual at a somewhat larger set of points than the number of free parameters used to represent the FB. This setup is perfectly suited for the *fminimax* routine, with the option set to minimize in max norm.

7. Numerical tests.

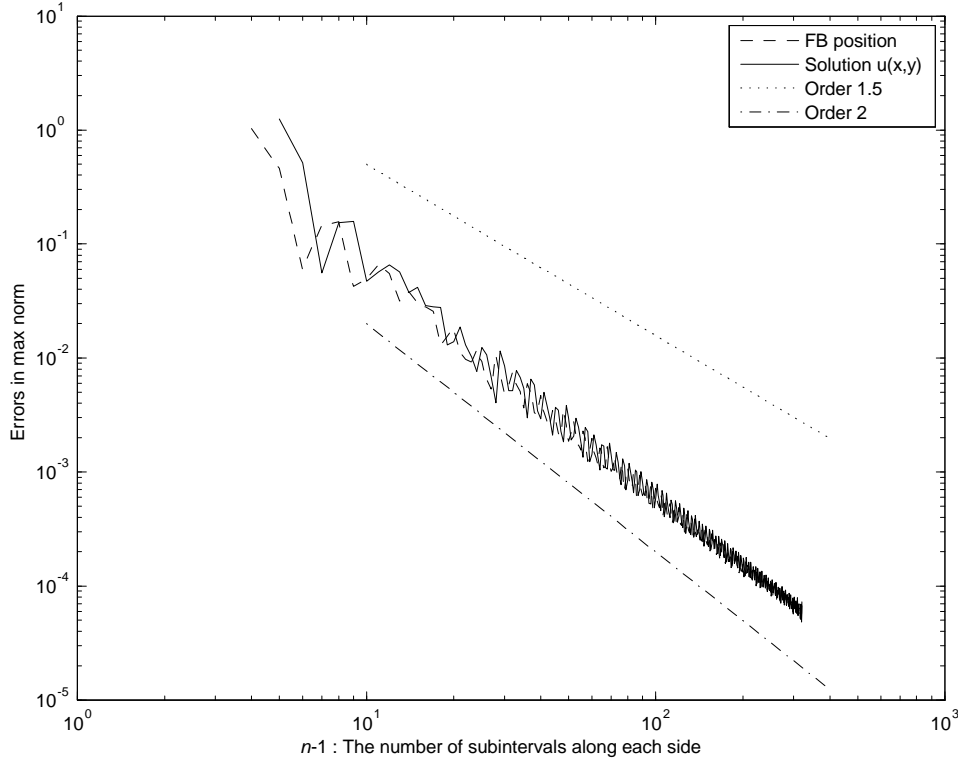


FIG. 7.1. Max norm errors in FB position and in solution $u(x,t)$ for the corrected FD2 scheme. The step size is $h = 8/(n-1)$. The lines marking the slopes $O(h^{1.5})$ and $O(h^2)$ are the same as in Figure 5.2.

7.1. Results for Problem 1. Figure 7.1 shows how the resulting errors both in FB position and for $u(x,y)$ (both in max norm, compared to the analytical results) vary with n . The procedure clearly solves the FB problem to full second order accuracy. We do not include any results here for the uncorrected FD2 scheme, since the residual then varies so erratically with small changes in FB position that *fminimax* either fails to converge, or becomes quite ineffective. With the correction procedure included, the *fminimax* procedure proved to be highly effective in terms of the number of function evaluations it requires. For its default error tolerance of 10^{-6} , it typically converges in 20-60 iterations (independently of n), each of which require no more than the solution of an FD2-discretized Poisson equation. A large number of effective Poisson solvers are readily available for this task. In the present work, we used sparse Gaussian elimination (as implemented through Matlab's "\ " operator), but any other standard approach, such as GMRES, multigrid solvers, etc., would also have worked perfectly well. When using sparse Gaussian elimination, the system can be *LU*-factorized once and for all, making the repeated solutions extremely fast. Iterative methods can utilize the fact that the solutions will differ very little between successive calls from the *fminimax* routine.

7.2. Results for Problem 2. There are three main differences compared to Problem 1:

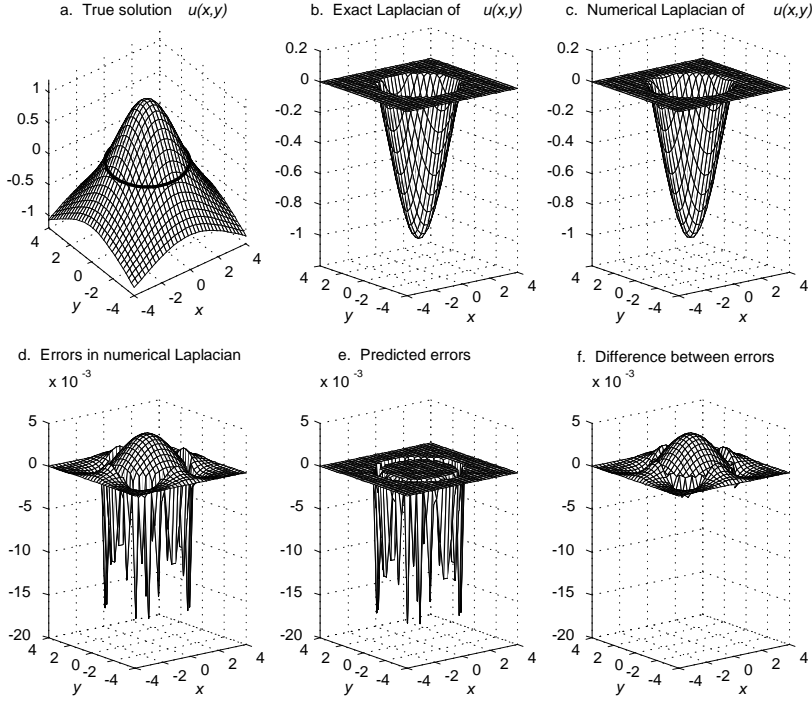


FIG. 7.2. The counterpart to Figure 4.1, but for Problem 2.

- Equation (3.2) becomes in this case replaced by

$$u_{\xi\xi} = \begin{cases} 0 & \text{where } \xi < 0 \\ -u & \text{where } \xi > 0 \end{cases} . \quad (7.1)$$

Further noting that u here can be closely approximated by $|\nabla u|\xi$ (with ∇u denoting the local gradient of u), the correction for any node k on the opposite side to the FB than the stencil center point becomes now $\frac{|\nabla u|}{6h^2}d_k^3$ instead of previously $\frac{1}{2h^2}d_k^2$.

- Some rough approximation (to within 1% or so) of $|\nabla u|$ is needed. This can readily be obtained by a solution of the FB problem with for example half the resolution of what we desire to use for our main solution.
- Another consequence of the $-u$ term in (7.1) is that the weight at the center point of the 5-point stencil becomes slightly modified for nodes inside the FB. Again, this is easily accommodated for by standard numerical Poisson solvers.

Figure 7.2 shows the same information for Problem 2 as what Figure 4.1 displayed for Problem 1. The errors in the (uncorrected) numerical Laplacian along the FB are

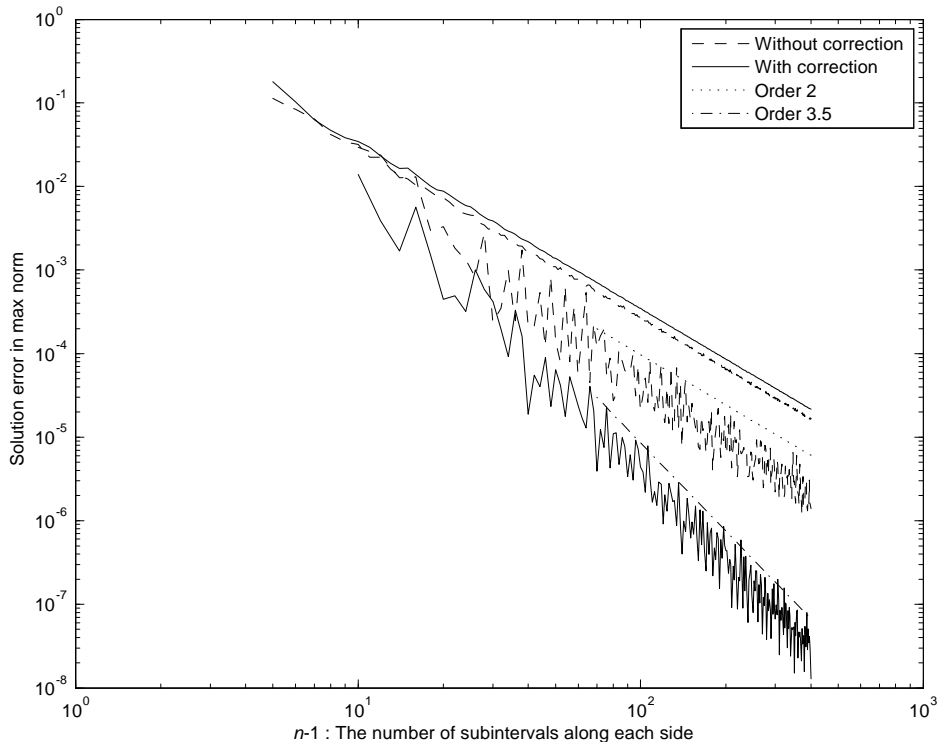


FIG. 7.3. Max norm errors when solving Problem 2 with the FB location given. The step size h satisfies $h = 8/(n-1)$. The top two curves show corrected and the uncorrected FD2 results. The two jagged curves show the previous results following a standard Richardson extrapolation. The trends for increasing n (decreasing h) seem now to agree well with $O(h^2)$ and $O(h^{3.5})$, respectively.

now much smaller in size (the solution $u(x, t)$ is discontinuous first in the third derivative, rather than in the second derivative for Problem 1) and they do not oscillate in sign. The correction scheme again provides excellent predictions for the FD2 scheme's errors along the FB and, with it eliminated, subplot (f) shows that regular truncation errors in the smooth regions then totally dominate any FB induced errors.

Figure 7.3 corresponds to Figure 5.2 for Problem 1. Even without the FB correction, the errors are on the $O(h^2)$ level. Because they are of one sign only (cf. Figure 7.2 d), they happen to partly balance out the errors seen in the center region. Hence we see in Figure 7.3 slightly smaller errors without the correction than with it (top two curves). However, there is a lot more fine-scale jitter in the uncorrected case, making Richardson extrapolation much less reliable. When we look at the extrapolated curves in Figure 7.3 (based on meshes with grid sizes h and $2h$), it becomes clear that the correction procedure combined with extrapolation is by far the most effective option.

The *fminimax* optimization applies again without any difficulties, producing accuracy results completely analogous to the residual results just shown in Figure 7.3.

7.3. Generalizations to other PDEs. The proposed correction procedure together with the use of *fminimax* generalizes immediately to the wider class of problems referred to in (1.1), (1.2), as well as to PDEs in more than two space variables. For details on generalizing the Laplacian to a general second order operator

$a(x, y) \frac{\partial^2 u}{\partial x^2} + b(x, y) \frac{\partial^2 u}{\partial x \partial y} + c(x, y) \frac{\partial^2 u}{\partial y^2}$, see for ex. equation (15) in [8]. Figures 8 and 9 in that reference show accuracy gains just as large as for the Laplacian case (for calculating the FD residual from a correct solution; that earlier work did not combine the correction procedure with any specific iterative solution scheme). Generalizations to 3-D are again immediate, with the only main issue the technicality of finding a suitable numerical representation of the free surface in terms of a relatively low number of parameters. In case this surface is approximately spherical in nature, an expansion in spherical harmonics will provide uniform resolution in the same way as a Fourier expansion does in 2-D polar coordinates.

8. Conclusions. We have in this study revisited a procedure that was first proposed in 1991 and which already then was shown to strongly reduce FD2 errors in the vicinity of a FB. It has now been combined with minimax optimization, producing an effective and easy-to-use approach for solving a wide range of FB problems. If the solution features a jump in the second derivative at the FB, full second order accuracy is obtained (in both solution and in the FB location). If the irregularity occurs first in the third derivative, Richardson extrapolation becomes available, and gives better than third order accuracy. In either case, the correction procedure greatly improves the accuracy of the original FD2 scheme or, if a certain accuracy level is required, this level may be reached with a fraction (maybe 1/100th or so) of the number of node points that otherwise would have been needed.

9. Acknowledgements. The present work was supported by the NSF Grants DMS-0611681, DMS-0914647 and ATM-0620068. The work was completed while the author was a Visiting Fellow at OCCAM (Oxford Centre for Collaborative Applied Mathematics) under support provided by Award No. KUK-C1-013-04, made by King Abdullah University of Science and Technology (KAUST).

REFERENCES

- [1] Bateman, G., MHD instabilities, MIT Press, Cambridge, MA / London (1980).
- [2] Borja, R.I. and Kishnani, S.S., On the solution of elliptic free-boundary problems via Newton's method, *Computer Math. in Appl. Mech. Eng.* 88 (1991), 341-361.
- [3] Crank, J., Free and moving boundary problems, Clarendon Press, Oxford (1984).
- [4] Elcrat, A., Fornberg, B., Horn, M. and Miller, K., Some steady vortex flows past a circular cylinder, *J. Fluid Mech.* 409 (2000), 13-27.
- [5] Fox, L. and Sankar, R., The regula-falsi method for free-boundary problems, *IMA J. Appl. Math.* 12 (1973), 49-54.
- [6] LeVeque, R.J. and Li, Z., The immersed interface method for elliptic equations with discontinuous coefficients and singular sources, *SIAM J. Numer. Anal.* 31 (1994), 1019-1044.
- [7] Miller, K., Fornberg, B., Flyer, N. and Low, B.C., Magnetic relaxation in the solar corona, *The Astrophysical Journal*, 609 (2009), 720-733.
- [8] Fornberg, B. and Meyer-Spasche, R., A finite difference procedure for a class of free boundary problems, *J. Comput. Phys.*, 102 (1992), 72-77.
- [9] Meyer-Spasche, R. and Fornberg, B., Discretization errors at free boundaries of the Grad-Schlüter-Shafranov equation, *Numer. Math.* 59 (1991), 683-710.
- [10] Scardovelli, R. and Zaleski, S., Direct numerical simulation of free-surface and interfacial flow, *Annual Rev. Fluid Mech.* 31 (1999), 567-603.

RECENT REPORTS

2009

01/09	A Mass and Solute Balance Model for Tear Volume and Osmolarity in The Normal And The Dry Eye	Gaffney Tiffany Yokoi Bron
02/09	Diffusion and permeation in binary solutions	Peppin
03/09	On the modelling of biological patterns with mechanochemical models: insights from analysis and computation	Moreo Gaffney Garcia-Aznar Doblare
04/09	Stability analysis of reaction-diffusion systems with time-dependent coefficients on growing domains	Madzvamuse Gaffney Maini
05/09	Onsager reciprocity in premelting solids	Peppin Spannuth Wettlaufer
06/09	Inherent noise can facilitate coherence in collective swarm motion	Yates <i>et al.</i>
07/09	Solving the Coupled System Improves Computational Efficiency of the Bidomain Equations	Southern Plank Vigmond Whiteley
08/09	Model reduction using a posteriori analysis	Whiteley
09/09	Equilibrium Order Parameters of Liquid Crystals in the Landau-De Gennes Theory	Majumdar
10/09	Landau-De Gennes theory of nematic liquid crystals: the Oseen-Frank limit and beyond	Majumdar Zarnescu
11/09	A Comparison of Numerical Methods used for Finite Element Modelling of Soft Tissue Deformation	Pathmanathan Gavaghan Whiteley
12/09	From Individual to Collective Behaviour of Unicellular Organisms: Recent Results and Open Problems	Xue Othmer Erban
13/09	Stochastic modelling of reaction-diffusion processes: algorithms for bimolecular reactions	Erban Chapman
14/09	Chaste: a test-driven approach to software development for physiological modelling	Pitt-Francis <i>et al.</i>

15/09	Block triangular preconditioners for PDE constrained optimization	Rees Stoll
16/09	From microscopic to macroscopic descriptions of cell migration on growing domains	Baker Yates Erban
17/09	The Influence of Gene Expression Time Delays on Gierer-Meinhardt Pattern Formation Systems	Seirin Lee Gaffney Monk
18/09	Analysis of a stochastic chemical system close to a sniper bifurcation of its mean field model	Erban <i>et al.</i>
19/09	On the existence and the applications of modified equations for stochastic differential equations	Zygalakis
20/09	Pebble bed: reflector treatment and pressure velocity coupling	Charpin <i>et al.</i>

Copies of these, and any other OCCAM reports can be obtained from:

**Oxford Centre for Collaborative Applied Mathematics
Mathematical Institute
24 - 29 St Giles'
Oxford
OX1 3LB
England
www.maths.ox.ac.uk/occam**